Available online at www.sciencedirect.com

SCIENCE DIRECT®

ELSEVIER

Journal of the European Ceramic Society 26 (2006) 2999–3004

www.elsevier.com/locate/jeurceramsoc

Synthesis, structure and oxygen thermally programmed desorption spectra of $La_{1-x}Ca_xAl_yFe_{1-y}O_{3-\delta}$ perovskites

Jaroslav Cihlar[a,b,*], David DelFavero[b], Jaroslav Cihlar Jr.[b], Antonín Buchal[a], Jan Van herle[c]

[a] Institute of Material Science and Engineering, Brno University of Technology, Technicka 2, 616 69 Brno, Czech Republic
[b] Institute of Material Chemistry, Brno University of Technology, Purkynova 118, 612 00 Brno, Czech Republic
[c] Laboratoire d'Energe'tique Industrielle, EPFL, CH-1015 Lausanne, Switzerland

Abstract

Perovskites $La_{1-x}Ca_xAl_yFe_{1-y}O_{3-\delta}$ (x, $y = 0$ to 1) were prepared by high-temperature solid-state synthesis based on mixtures of oxides produced by colloidal milling. The XRD analysis showed that perovskites $La_{0.5}Ca_{0.5}Al_yFe_{1-y}O_{3-\delta}$ with a high Fe content ($1 - y = 0.8$–1.0) were of orthorhombic structure, perovskites with a medium Fe content ($1 - y = 0.8$–0.5) were of rhombohedral structure, and perovskite with the lowest Fe content ($1 - y = 0.2$) were of cubic structure. Thermally programmed desorption (TPD) of oxygen revealed that chemical desorption of oxygen in the temperature range from 200 to 1000 °C had proceeded in the two desorption peaks. The low-temperature α-peak (in the 200–550 °C temperature range) was brought about by oxygen liberated from oxygen vacancies; the high-temperature β-peak (in the 550–1000 °C temperature range) corresponded to the reduction of Fe^{4+} to Fe^{3+}. The chemidesorption oxygen capacity increased with increasing Ca content and decreased with increasing Al content in the perovskites. The Al^{3+} ions restricted, probably for kinetic reasons, the reduction of Fe^{4+} and the high-temperature oxygen desorption associated with it.

Keywords: Perovskites; Membranes; X-ray methods; Powders-solid state reaction; Chemisorption

1. Introduction

Multi-component oxide phases with the perovskite structure and mixed ionic and electronic conductivities find a broad application as cathodes in fuel cells (solid oxide fuel cell—SOFC) or as membranes with high oxygen permeability in membrane reactors and devices for separation of oxygen. Significant catalytic applications of these perovskites include reactors for partial and total oxidation of hydrocarbons and in devices for the removal of pollutants from combustion gases.[1,2] Perovskites for ceramic membranes in particular must meet a number of requirements such as thermodynamic and dimensional stability in oxidation and reduction atmospheres, high oxygen permeability, and electrochemical compatibility with catalysts and electrolytes.[3]

In recent years increased attention has been paid to low cost $LaFeO_3$ perovskites doped with Sr, which have high ionic and electronic conductivities and considerable oxygen permeability. But these perovskites have insufficient thermodynamic and dimensional stability at high oxygen gradients that occur in membrane reactors.[3]

The stability of the $La_{1-x}Sr_xFeO_{3-\delta}$ perovskites is increased by isovalent doping of Fe cations by $A1^{3+}$ which are stable in a redox medium.[3–5] Doping $La_{1-x}Sr_xFeO_{3-\delta}$ by Al^{3+} ions leads simultaneously to reducing the perovskite conductivity.[6] Measuring the conductivity of $La_{1-x}Sr_xFeO_{3-\delta}$ perovskites yielded information about the relation between the structure of perovskites and their electrical properties, which are important for solid oxide fuel cell applications in particular. Of equal importance for catalytic and membrane applications are data on the chemisorption behaviour of perovskites in an oxidation–reduction medium. Seiyama found that when the $LaSrBO_3$ perovskites were heated to a high temperature, oxygen was liberated in two desorption peaks.[7] In the TPD spectra, a low-temperature peak, denoted as α, appeared in the 300–600 °C temperature range while a high-temperature peak, denoted as β, appeared in the 600–900 °C temperature range. While the α-peak resulted from the liberation of oxygen bonded in superficial oxygen vacancies, the β-peak was related to the ion reduction

---

[*] Corresponding author. Tel.: +420 5 41143383; fax: +420 5 41153202.
E-mail address: cihlar@fme.vutbr.cz (J. Cihlar).

0955-2219/$ – see front matter © 2006 Elsevier Ltd. All rights reserved.
doi:10.1016/j.jeurceramsoc.2006.02.018

of transition metal B in the perovskites. Since the β oxygen was desorbed from interfacial species, its liberation in the thermal way was more difficult than the liberation of the α oxygen.[8] The amount of oxygen liberated in the region of both the α-peak and the β-peak increased with the concentration of the dopant (Sr^{2+} ions), i.e., with increasing concentration of oxygen vacancies in the perovskite. While the preparation, structure and properties of La–Sr–Fe–Al–O perovskite systems has been the subject of several in-depth publications, information on the analogous La–Ca–Fe–Al–O system is practically non-existent. The present work therefore focuses on the synthesis, structure and chemisorption properties of the $La_{1-x}Ca_xFe_yAl_{1-y}O_{3-\delta}$ perovskite system.

2. Experimental

2.1. Materials

In the synthesis of perovskites the following powder oxides were used: CaO (p.a., Lachema, Czech Republic), La_2O_3 (purity 99.99%, Verochem, Czech Republic), Fe_2O_3, Al_2O_3 (p.a., ML Chemica, Czech Republic), MnO (p.a., Aldrich, Germany). The dispersion medium used was isopropanol, xylene (p.a., Czech Republic), acetone (p.a., Penta, Czech Republic), and distilled water. Oleic acid and monochloroacetic acid (p.a., Aldrich, Germany) were used as surface-active substances.

2.2. Preparation of perovskites

The oxides, the weight proportions of which were chosen such as to cover the La:Ca:Fe:Al molar ratios in the range from 0 to 1.0, were mixed and milled in liquid medium in the presence of additives (oleic acid or monochloroacetic acid) in a laboratory attritor of 600 ml capacity, filled with balls of tetragonal ZrO_2, at 200 revolutions/min for a period of 4–16 h. In the initial stage, four liquid media were tested: isopropanol, acetone, xylene, and water. Acetone was found to be the most suitable liquid medium for colloidal milling since in this medium the milled mixtures of oxides had a large specific surface area (ca. 20 m^2/g) already after 8 h of milling (see Fig. 1), and the oxides in acetone did not hydrolyze (in contrast to the aqueous medium). Colloidal milling of the mixtures of oxides in the preparation of the $La_{1-x}Ca_xAl_yFe_{1-y}O_{3-\delta}$ perovskites was conducted in acetone for a period of 8 h. The milled suspensions were centrifuged, washed in isopropanol, and dried at a temperature of 120 °C. The dried powders were subjected to solid-state reaction in air atmosphere at a temperature of 1450 °C for a period of 24 h.

2.3. Analysis of products

The phase composition of the products was established by X-ray diffraction analysis (X'pert, Philips, the Netherlands), and the lattice parameters were determined using Rietveld analysis.[9] The shape and size of particles were determined via scanning electron microscopy (XL, 30, Philips, the Netherlands). The chemical analysis of perovskites was performed on microprobe attached to the electron microscope and by IPS/AES spectroscopy (JY 170 Ultrace, Jobin-Yvon, France). The specific surface area of powder perovskites was established by the BET method on a Chembet-3000 instrument (Quantachrome, USA).

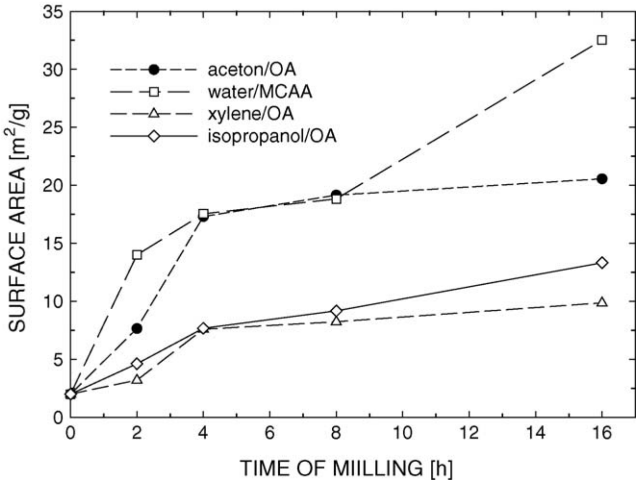

Fig. 1. Dependence of specific surface on the time of milling powder oxides and the type of liquid medium.

The thermally programmed oxygen spectra (TPR, TPO) were also measured on a Chembet-3000 instrument (Quantachrome, USA).

The measurement of TPD and TPO spectra was conducted in three steps:

(a) Reduction of perovskite in a He + 5%H_2 atmosphere in a temperature range of 20–1100 °C at a heating rate of 20 °C/min, and cooling the reduced perovskite to 20 °C.
(b) Oxidation of perovskite in oxygen atmosphere under the same conditions as in step (a).
(c) Desorption of oxygen from oxidized perovskite under the same conditions as in step (a).

2.4. Stability of perovskite systems

For the prediction of the stability of perovskite systems of the type of $La_{1-x}Ca_xFe_yAl_{1-y}O_{3-\delta}$, Goldschmidt's tolerance factor t[10] was used, expressed by the Eq. (1)

$$t = \frac{(xr_{Ca} + (1-x)r_{La} + r_o)}{\sqrt{2}(yr_{Fe} + (1-y)r_{Al} + r_o)} \quad (1)$$

where r_{La} and r_{Ca} are the ion radii of the elements La an Ca [nm]; r_{Fe} and r_{Al} are the ion radii of the elements Fe and Al, and r_o is the ion radius of oxygen. The values of ionic radii were taken over from.[11,12]

3. Results and discussion

It can be seen from Fig. 1 that in the La–Ca–Al–Fe–O perovskite system, 13 basic mixtures were used but only six single-phase perovskites and one brownmillerite of the composition given in Table 1 were prepared. In the remaining six cases, multiphase products were produced. In view of the fact that over the whole concentration range of components (CaO, La_2O_3, Fe_2O_3,

Table 1
Phase compositions and crystallographic data for the La–Ca–Al–Fe–O ceramic system

Composition (input)	Phase composition (XRD analysis)	Space group	Unit cell parameters (nm)			Crystalographic density (g/cm^3)
			a	*b*	*c*	
$La_{0.5}Ca_{0.5}FeO_3$	Perovskite-orthorhombic phase	*Pbnm*	0.547076	0.546458	0.772702	5.74
$CaAl_{0.5}Fe_{0.5}O_3$	Browmillerite-orthorhombic phase	*Ibm*2				
$La_{0.5}Ca_{0.5}AlO_3$	85% Perovskite + $LaCaAl_3O_7$					
$LaAl_{0.5}Fe_{0.5}O_3$	Perovskite-rhombohedral phase	*R3cH*	0.547990	0.547990	1.329590	6.31
$La_{0.8}Ca_{0.2}Al_{0.2}Fe_{0.8}O_3$	Perovskite-orthorhombic phase	*Pbnm*	0.549104	0.550308	0.776773	5.94
$La_{0.8}Ca_{0.2}Al_{0.5}Fe_{0.5}O_3$	85% Perovskite + $LaCaAl_3O_7$					
$La_{0.8}Ca_{0.2}Al_{0.8}Fe_{0.2}O_3$	76% Perovskite m-La_2O_3					
$La_{0.5}Ca_{0.5}Al_{0.2}Fe_{0.8}O_3$	Perovskite-orthorhombic phase	*Pbnm*	0.549209	0.545915	0.772702	5.22
$La_{0.5}Ca_{0.5}Al_{0.5}Fe_{0.5}O_3$	Perovskite-rhombohedral phase	*R3cH*	0.544096	0.544096	1.326203	5.04
$La_{0.5}Ca_{0.5}Al_{0.8}Fe_{0.2}O_3$	Perovskite-cubic phase	*Pm*3*m*	0.381736	0.381736	0.381736	4.94
$La_{0.2}Ca_{0.8}Al_{0.2}Fe_{0.8}O_3$	60% $Ca_4Al_{0.48}Fe_{1.52}O_5$ – brownmillerite + 10% $Ca_2Al_{0.6}Fe_{1.4}O_5$ + 10% $Fe_2Ca_2O_5$ + 20% $LaCaAl_3O_7$					
$La_{0.2}Ca_{0.8}Al_{0.5}Fe_{0.5}O_3$	50% $Ca_2Al_{0.48}Fe_{1.52}O_5$ – brownmillerite + 10% $Ca_2Al_{0.6}Fe_{1.4}O_5$ + 10% $CaFe_4O_6$ + 30% $LaCaAl_3O_7$					
$La_{0.2}Ca_{0.8}Al_{0.8}Fe_{0.2}O_3$	10% $Ca_3Al_2Fe_2O_6$ + 80% $Ca_3Al_2O_6$ + 10% $LaCaAl_3O_7$					

Al_2O_3) the tolerance factors were close to the value 1 (0.99–1.0) (see Fig. 2), stable single-phase perovskites should, theoretically, be formed in all the cases.[13] Why this did not happen can be explained by kinetics reasons.[3,14] Colloidal milling probably did not, in all cases, lead to sufficient homogenization of initial substances (oxides) and so under conditions of high-temperature solid-state reaction, which is controlled by ion diffusion in solid state, the reaction did not proceed homogenously to the formation of single-phase product—the perovskite. This explanation is acceptable in the case of perovskites doped with a low concentration of Sr^{2+} ions (molar ratio La:Ca = 0.8:0.2). But as can be seen from Table 1, the solid-state reaction was affected by the chemical composition of reactants. Single-phase perovskite formed most easily at a molar ratio of La:Ca = 0.5:0.5. At a molar ratio of La:Ca = 0.2:0.8 brownmillerites and binary or ternary oxides were formed. The content of Ca at a molar ratio of La:Ca = 0.2:0.8 probably limited the solubility of Al^{3+} ions in the Fe sublattice and prevented the formation of perovskite phases. From this viewpoint, the La–Ca–Al–Fe–O system behaved like the La–Sr–Al–Fe–O system or the La–Sr–Al–Ga–O system, in which no perovskite phases containing more than 40% Al^{3+} or 31% Ga^{3+} respectively, and high content of Sr^{2+} ions were prepared.[3,15] The results given in this part of the work are primarily based on the study of pure perovskite phases of the type of $La_{0.5}Ca_{0.5}Fe_yAl_{1-y}O_{3-\delta}$.

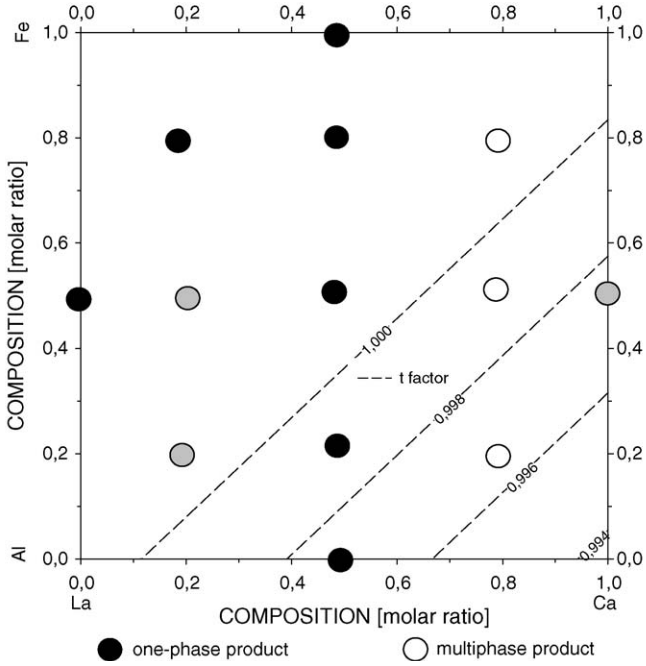

Fig. 2. Tolerance factors for the La–Ca–Al–Fe–O ceramic system.

It follows from the X-ray diffraction spectra of the $La_{0.5}Ca_{0.5}Fe_yAl_{1-y}O_{3-\delta}$ perovskites given in Fig. 3 and, in particular, Table 1, that the crystallographic space group of perovskites depended in the first place on the content of Fe ions in the crystal lattice. Perovskites with a high Fe content ($y = 0.8$ to 1.0) crystallized in orthorhombic structure with *Pbnm* space group, perovskites with a medium Fe content ($y = 0.5$) in rhombohedral structure with R3c spatial group, and the perovskite with the lowest Fe content ($y = 0.2$) in cubic structure with *Pm*3*m*

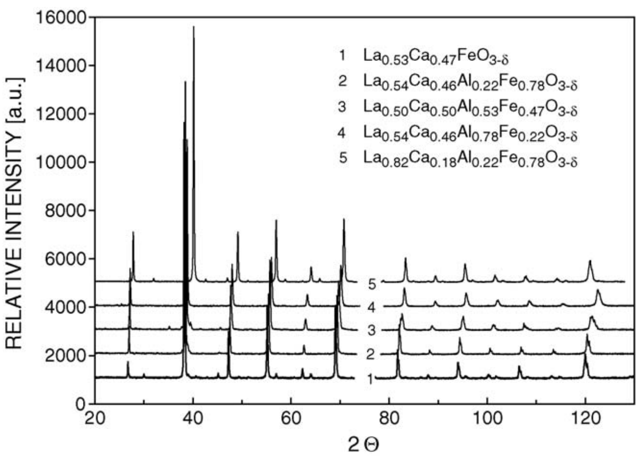

Fig. 3. XRD spectra of the $La_{1-x}Ca_xAl_yFe_{1-y}O_{3-\delta}$ perovskites.

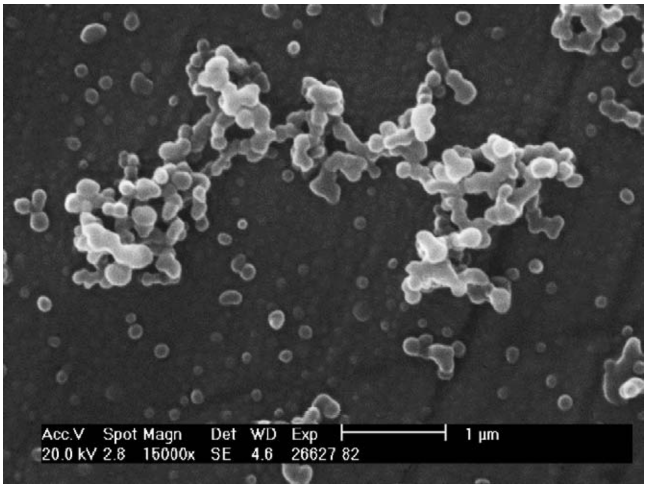

Fig. 4. Morphology of $La_{0.54}Ca_{0.46}Al_{0.78}Fe_{0.22}O_{3-\delta}$ particles according to SEM.

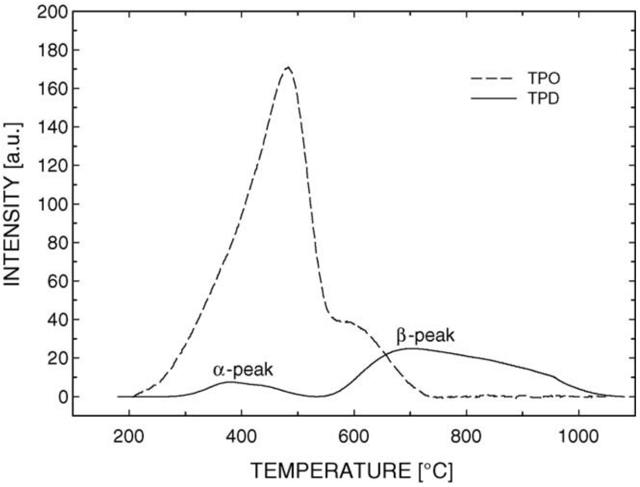

Fig. 5. Oxygen TPD and TPO spectra of the $La_{0.54}Ca_{0.46}Al_{0.22}Fe_{0.78}O_{3-\delta}$ perovskite.

space group. As expected, the theoretical (crystallographic) density of the perovskites with constant ratio La:Ca = 0.5 increased with increasing Fe content in the lattice (4.94–5.74 g/cm^3). A typical morphology of the $La_{0.5}Ca_{0.5}Fe_yAl_{1-y}O_{3-\delta}$ perovskite particles can be seen in Fig. 4. The primary particles were about 200 nm in size and formed agglomerates larger than 1.0 μm. The composition of perovskites as established by EDX and ICP analysis is given in Table 2. The analysed perovskite composition given in Table 2 exhibits slight deviations from the composition calculated from the weighted amounts of input reactants. The likely cause is the loss of reactants during the preparation of perovskites.

The thermally programmed spectra (TPO and TPD) of the $La_{0.54}Ca_{0.46}Al_{0.22}Fe_{0.78}O_3$ perovskite given in Fig. 5 contain information on the oxygen exchange capacity of perovskite in an oxidizing and inert He atmosphere. It follows from Fig. 5 that in the temperature range from 200 to 1000 °C the perovskite exchanged about four times as much oxygen in the oxidizing regime (TPO) than in thermal desorption (TPD). The volume of exchanged gas (O_2) exceeded by more than two orders the amount of surface adsorbed gas (related to the specific surface of perovskites, which was 1.5–2 m^2/g). In the TPO and TPD processes, oxygen was exchanged by the chemisorption mechanism, in which ions participated not only on the surface of but also inside the perovskite. Although the combination of TPO and TPD spectra yields complete information about the redox properties of perovskites, the present work is, for practical reasons, based on only TPD spectra. In the TPD spectra of the La–Ca–Al–Fe–O perovskite systems two characteristic peaks can be seen (see Fig. 6). One peak, denoted α-, lies in the 200–550 °C range, the other peak, denoted β-, lies in the 550–1000 °C range. From Table 3 it follows that the total amount of oxygen liberated from the perovskite depended on the content of dopant at point A of the crystal lattice of perovskite (Ca) and on the Fe content at point B. At a La:Ca molar ratio of ca. 0.5:0.5 the total amount of liberated oxygen increased with increasing Fe concentration. The amount of liberated oxygen in the 200–550 °C temperature range (α peak) was practically independent of the Fe content in perovskite. The growing Fe content in perovskite was shown by the growth of oxygen liberated in the temperature region from 550 to 1000 °C (β peak). The TPD spectra of the La–Ca–Al–Fe–O perovskites are similar to the TPD spectra of the La–Sr–Co–O or La–Sr–Fe–O systems and thus also the mechanism of oxygen chemisorption will probably be similar and have these features:[7]

(a) Due to the substitution of La^{3+} ions by calcium in the crystal lattice (at point A) of the basic $LaFeO_3$ perovskite oxygen vacancies (V_o) are formed.

Table 2
Theoretical and analysed compositions for $La_{1-x}Ca_xAl_yFe_{1-y}O_{3-\delta}$ perovskites

Teoretical composition (input)	Experimental composition (analysed)
$La_{0.50}Ca_{0.50}FeO_3$	$La_{0.53}Ca_{0.47}FeO_3$
$CaAl_{0.50}Fe_{0.50}O_3$	$Ca_{0.93}Al_{0.49}Fe_{0.51}O_3$
$La_{0.80}Ca_{0.20}Al_{0.20}Fe_{0.80}O_3$	$La_{0.82}Ca_{0.18}Al_{0.22}Fe_{0.78}O_3$
$La_{0.50}Ca_{0.50}Al_{0.20}Fe_{0.80}O_3$	$La_{0.54}Ca_{0.46}Al_{0.22}Fe_{0.78}O_3$
$La_{0.50}Ca_{0.50}Al_{0.50}Fe_{0.50}O_3$	$La_{0.50}Ca_{0.50}Al_{0.53}Fe_{0.47}O_3$
$La_{0.50}Ca_{0.50}Al_{0.80}Fe_{0.20}O_3$	$La_{0.54}Ca_{0.46}Al_{0.78}Fe_{0.22}O_3$

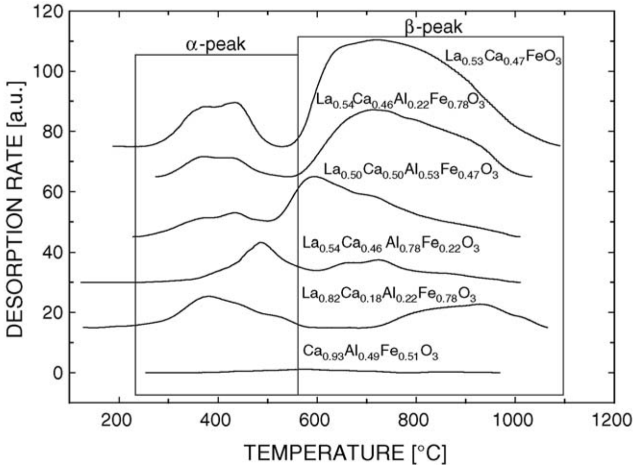

Fig. 6. Oxygen TPD spectra of $La_{1-x}Ca_xAl_yFe_{1-y}O_{3-\delta}$ perovskites.

Table 3
Oxygen TPD analysis of $La_{1-x}Ca_xAl_yFe_{1-y}O_{3-\delta}$ perovskites

Perovskite	O_2 Desorption ($\frac{\text{mol } O_2}{\text{g perovskite}}$)			O_2 Desorption ($\frac{\text{mol } O_2}{\text{mol perovskite}}$)			O_2 Desorption ($\frac{\text{mol } O_2}{\text{mol Fe}}$)		
	Σ	α-Peak %	β-Peak %	Σ	α-Peak	β-Peak	Σ	α-Peak	β-Peak
$La_{0.53}Ca_{0.47}FeO_{3-\delta}$	4.03×10^{-4}	16.0	84.0	0.079	0.013	0.067	0.079	0.013	0.066
$La_{0.54}Ca_{0.46}Al_{0.22}Fe_{0.78}O_{3-\delta}$	3.07×10^{-4}	13.6	86.4	0.058	0.008	0.0504	0.0755	0.0102	0.0653
$La_{0.5}Ca_{0.5}Al_{0.53}Fe_{0.47}O_{3-\delta}$	1.66×10^{-4}	22.0	78.0	0.030	0.0065	0.023	0.063	0.014	0.049
$La_{0.54}Ca_{0.46}Al_{0.78}Fe_{0.22}O_{3-\delta}$	9.13×10^{-5}	50.7	49.3	0.016	0.0081	0.0079	0.050	0.0137	0.036
$La_{0.82}Ca_{0.18}Al_{0.22}Fe_{0.78}O_{3-\delta}$	1.04×10^{-4}	50.8	49.2	0.023	0.012	0.011	0.029	0.015	0.014
$Ca_{0.93}Al_{0.49}Fe_{0.51}O_{3-\delta}$	7.68×10^{-6}	91.5	8.5	0.009	0.0089	0.00008	0.002	0.0018	0.00016

(b) The 3d-transition metal (Fe) at point B of the perovskite crystal lattice may increase its oxidation number by oxidation and reduce it by reduction according to Eq. (2)

$$Fe^{3+} = Fe^{4+} + e^- \tag{2}$$

(c) In the oxidation of the perovskite, oxidation of transition metal and chemisorption of oxygen into the crystal lattice can take places of oxygen vacancies.

(d) During thermal desorption in an inert atmosphere, oxygen from oxygen vacancies (α-peak, 200–550 °C) is the first to be liberated.

(e) At temperatures exceeding 550 °C the transition metal is reduced under simultaneous oxygen liberation from the crystal lattice (β-peak).

The above mechanism is confirmed by the results obtained (see Table 3): with decreasing substitution of La^{3+} by calcium at point A the amount of desorbed oxygen decreased, the same as with the decreasing Fe concentration at point B. Ca acted as active dopant at point A. On the basis of data from the literature it was expected that doping Fe at point B by aluminium would increase perovskite stability in the oxidation–reduction atmosphere, but it did not affect the redox behaviour of Fe.[3–5] However, it was found that the Al^{3+} ions were not inert but affected the chemisorption of oxygen in perovskite. Fig. 7 gives the dependence of the amount of oxygen liberated in the low-temperature and the high-temperature regions of TPD spectra of the $La_{0.5}Ca_{0.5}Fe_yAl_{1-y}O_{3-\delta}$ perovskites (α and β peaks) on the Al^{3+} content. The total amount of oxygen liberated from the perovskite in the temperature range 20–1000 °C dropped from 0.08 to 0.01 mol/mol of perovskite with Al^{3+} concentration increasing from 0 to 0.8 mol/mol of perovskite. The Al content had practically no effect on the oxygen liberated from oxygen vacancies (α-peak), it only affected the amount of oxygen liberated by the reduction of Fe^{4+} ions (β-peak). The effect of Al^{3+} ions can better be seen in Fig. 8, where the amount of liberated oxygen is related to the Fe in the perovskite. After the substitution of 80% of Fe by aluminium the chemidesorbed amount of high-temperature oxygen related to 1 mol of Fe dropped to almost one half (from 0.066 to 0.036 mol O_2/mol Fe). Since in the course of the liberation of high-temperature oxygen there is a reduction of Fe^{4+} ions, Al^{3+} ions in the perovskite lattice limit the Fe^{4+} to Fe^{3+} reduction. The reason for this limitation probably controls the kinetics of the redox process. At low concentrations of Fe^{4+} ions in the Fe sublattice containing numerous doping Al^{3+} ions the oxidation and reduction of Fe ions proceed slowly and take a long time to reach equilibrium. This certainly has no effect on perovskite conductivity as the Al^{3+} ions did not affect oxygen liberation from oxygen vacancies and thus they did not affect their concentration either, but it undoubtedly

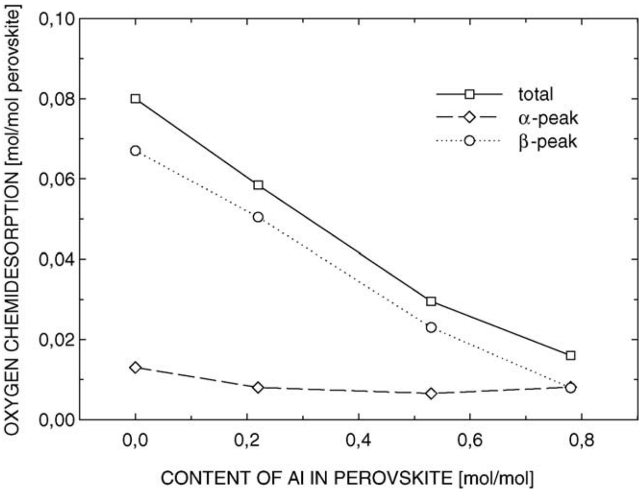

Fig. 7. Effect of aluminium content on oxygen desorption in the $La_{0.5}Ca_{0.5}Al_yFe_{1-y}O_{3-\delta}$ perovskites (related to one mole of perovskite).

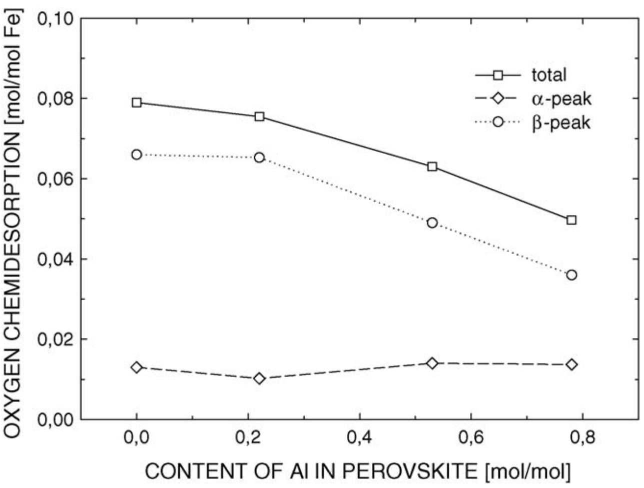

Fig. 8. Effect of aluminium content on oxygen desorption in the $La_{0.5}Ca_{0.5}Al_yFe_{1-y}O_{3-\delta}$ perovskites (related to one mole of Fe).

has an effect on the oxygen exchange capacity in perovskite membranes.

4. Conclusions

High-temperature solid-state synthesis of the $La_{1-x}Ca_xAl_yFe_{1-y}O_{3-\delta}$ (x, $y = 0$ to 1) perovskites, based on a mixture of oxides prepared by colloidal milling led to single-phase perovskites of the type of $La_{0.5}Ca_{0.5}Al_yFe_{1-y}O_{3-\delta}$, whose crystal structure depended on Fe content. Perovskites with a high Fe content ($1 - y = 0.8$–1.0) were of orthorhombic structure, perovskites with a medium Fe content ($1 - y = 0.5$) had a rhombohedral structure, and perovskites with the lowest Fe content ($1 - y = 0.2$) had a cubic structure. The perovskites contained oxygen vacancies formed by the substitution of La by calcium, and had a considerable chemidesorption capacity in an inert atmosphere (He). Oxygen chemidesorption in the temperature range from 200 to 1000 °C proceeded in the two systems in two desorption peaks. The α-peak in the 200–500 °C temperature range was due to the liberation of oxygen from oxygen vacancies, the β-peak (in the 550–1000 °C temperature range) corresponded to the reduction of d-transition metal (Fe^{4+}). The chemidesorption capacity of oxygen increased with increasing Ca content, and decreased with increasing Al content in the perovskites. The Al^{3+} ions reduced, probably for kinetic reasons, the high-temperature desorption of oxygen (β-peak) associated with the reduction of Fe^{4+}.

Acknowledgements

Part of this work was performed within the project "COST 525.10". The financial support of Ministry of Education, Sport and Health of Czech Republic is gratefully acknowledged.

References

1. Tejuca, L. G. and Fiero, J. L. G., ed., *Properties and applications of perovskite-type oxides*. Marcel Dekker, New York, 1993.
2. Schaak, R. E. and Mallouk, T. E., Perovskite by design: a toolbook of solid-state reactions. *Chem. Mater.*, 2002, **14**, 1455–1471.
3. Yaremchenko, A. A., Patrakeev, M. V., Kharton, V. V., Marques, F. M. B., Leonidov, I. A. and Kozhevnikov, V. L., Oxygen ionic and electronic conductivity of $La_{0.3}Sr_{0.7}Fe(Al)O_{3-\delta}$ perovskites. *Solid State Sci.*, 2004, **6**, 357–366.
4. Kuščer, D., Hanžel, D., Hrovat, M., Holc, J. and Kolar, D., Defect structure and electrical properties of $La_{1-y}Sr_yFe_{1-x}Al_xO_{3-\delta}$. *J. Am. Ceram. Soc.*, 2001, **84**, 1148–1154.
5. Kuščer, D., Hrovat, M., Holc, J., Bernik, S. and Kolar, D., Electrical and microstructural characterization of Al_2O_3 doped $LaFeO_3$. *J. Mater. Sci. Lett.*, 1996, **15**, 974–977.
6. Holc, J., Kuščer, D., Hrovat, M., Bernik, S. and Kolar, D., Electrical and microstructural characterisation of $(La_{0.8}Sr_{0.2})(Fe_{1-x}Al_x)O_3$ and $(La_{0.8}Sr_{0.2})(Mn_{1-x}Al_x)O_3$ as possible SOFC cathode material. *Solid State Ionics*, 1997, **95**, 259–268.
7. Seiyama, T., Total oxidation of hydrocarbons on perovskite system. In *Properties and applications of perovskite-type oxides*, ed. L. G. Tejuca. Marcel Dekker, New York, 1993, pp. 215–234.
8. Fino, D., Russo, N., Saracco, G. and Specchia, V., The role of suprafacial oxygen in some perovskites for catalytic combustion of soot. *J. Catal.*, 2003, **217**, 367–375.
9. Rietveld, H. M., A profile refinement method for nuclear and magnetic structures. *J. Appl. Cryst.*, 1969, **2**, 65–71.
10. Trofimenko, N. and Ullmann, H., Transition metal doped lanthanum gallates. *Solid State Ionics*, 1999, **118**, 215–227.
11. Yamamura, Y., Ihara, Ch., Kawasaki, S., Sakai, H., Suzuki, K., Takami, S. *et al.*, Materials design of perovskite-based oxygen ion conductor by molecular dynamics method. *Solid State Ionics*, 2003, **160**, 93–101.
12. Shannon, R. D., Revised effective ionic radii and systematic studies of interatomic distance in halides and chalcogenides. *Acta Cryst.*, 1976, **A32**, 751–755.
13. Hayashi, H., Inaba, H., Matsuyama, M., Lan, N. G., Dokiya, M. and Tagawa, H., Structural consideration on the ionic conductivity of perovskite-type oxides. *Solid State Ionics*, 1999, **122**, 1–15.
14. Waerenborgh, J. C., Dojas, D. P., Vyshatko, N. P., Shaula, A. L., Karton, V. V., Marozau, I. P. *et al.*, Fe^{4+} formation in brownmillerite $CaAl_{0.5}Fe_{0.5}O_{2.5+\delta}$. *Mater. Lett.*, 2003, **57**, 4388–4393.
15. Karton, V. V., Shaula, A. L., Viskup, A. P., Avdeeva, M., Yaremchenko, A. A., Patrakeev, M. V. *et al.*, Perovskite-like system (Sr,La)(Fe,Ga)$O3_{-\delta}$: structure and ionic transport under oxidizing conditions. *Solid State Ionics*, 2002, **150**, 229–243.